Imaging bandwidth of the tapping mode atomic force microscope probe

János Kokavecz,[1,*] Othmar Marti,[2] Péter Heszler,[3,4] and Ádám Mechler[5,†]
[1]*Department of Optics and Quantum Electronics, University of Szeged, P.O. Box 406, H-6701 Szeged, Hungary*
[2]*Department of Experimental Physics, University of Ulm, Albert-Einstein-Allee 11 D-89069 Ulm, Germany*
[3]*Research Group on Laser Physics of the Hungarian Academy of Sciences, P.O. Box 406, H-6701 Szeged, Hungary*
[4]*The Ångström Laboratory, Department of Engineering Sciences, Uppsala University, Box 534, SE-75121 Uppsala, Sweden*
[5]*School of Chemistry, Monash University, Clayton, VIC 3800, Australia*
(Received 15 June 2005; revised manuscript received 29 November 2005; published 4 April 2006)

In this work we report a comprehensive experimental and computational study of the dynamical behavior of the tapping mode atomic force microscope (AFM) probe in interaction with the force field of a sample surface. To address the nonlinear nature of the probe dynamics, we apply describing function method. We established that the corner frequency of the low pass describing function of the probe is sensitive to the modulation amplitude and is generally higher than predicted by linear — force gradient — approximation. We show that large tip apex radii and high values of surface Young's moduli can introduce a resonant amplitude transfer, which could lead to image distortion and system instabilities. We demonstrate that the oscillating amplitude of the probe far from the surface and during imaging, and the ratio of these two (setpoint) have an influence on the describing function of the probe similar to that of the quality factor. Accordingly, expert control of these parameters is as effective as active Q control in improving the imaging bandwidth of the tapping mode AFM.

DOI: 10.1103/PhysRevB.73.155403 PACS number(s): 68.37.Ps, 07.79.Lh

I. INTRODUCTION

Atomic force microscopy (AFM) has evolved into a routine tool for characterizing nanostructured surfaces since the invention of the method nearly two decades ago.[1] The principle of operation is simple and straightforward: a scanning cantilevered tip (probe) provides a signal for mapping the surface, sliding over the features in contact, or tapping along the structures with a presumably sinusoidal motion in tapping mode. To avoid surface damage, the probe signal — bending or amplitude — is maintained constant *via* controlling the probe-surface distance through a feedback mechanism. A continuous stream of theoretical and experimental works on the improvement and interpretation of subnanometer imaging indicates, however, that the simplicity does not apply to the acquisition and interpretation of high resolution AFM images (e.g., Refs. 2–9). Tapping mode, in particular, is prone to instabilities and inconsistencies when imaging on the nanometer scale. On one hand, the amplitude of the oscillating probe is a complex function of the material properties of the sample, the cantilevered tip and the environment; even in equilibrium state, this complexity results in systematic errors — imaging artifacts — inherent to the process.[2,3,5–9] In nonequilibrium state, like the AFM in operation, this complexity can cause nonlinear and even chaotic behavior.[10–12] On the other hand, the narrow imaging bandwidth of the tapping mode operation poses the dilemma of sacrificing the surface tracking (contrast) and the reproducibility of the images for higher frame capture rates or *vice versa*.[11–13] The nonlinearities of the interaction might also interfere with the dynamical behavior of the probe; it is thus feasible to study the imaging bandwidth in consideration of realistic working conditions.

The imaging bandwidth is a product of the transfer functions of all components placed in the feedback loop. For the (nonoscillating) probe it falls into the range of several hundred kHz which would provide reliable surface tracking for practically all imaging conditions.[10] The bandwidth of the piezo actuator and the feedback loop ("hardware"), however, is of the order of several kHz.[10] Recent works have shown that significant improvement can be achieved by applying faster piezoceramics,[14] integrating the piezo actuator onto the cantilever,[15–17] improving the data acquisition speed and also by introducing advanced control algorithms.[18,19] Altogether, these solutions lead to an almost two orders of magnitude improvement in imaging bandwidth. In contrast, due to inherent mechanical properties of the probe, in particular, the slew rate when following a surface modulation and transients generated by step function perturbations, the bandwidth of the tapping mode probe is restricted to a few kHz.[12,13]

Analytical modeling of the tapping mode often relies on the force gradient approximation, assuming that the tip-sample interaction force is linear and thus it can be considered as a modified cantilever spring constant. Using the force gradient approximation, Mertz, Marti, and Mlynek[13] derived that the tapping mode probe is a linear system with a simple transfer function. It has a low pass transfer character with a −3 dB bandwidth (Ω) in the form of

$$\Omega = \frac{\omega_0}{2Q} \tag{1}$$

provided that the probe is driven at its resonance frequency. In Eq. (1), ω_0 and Q denote the undamped angular resonance frequency and quality factor of the probe, respectively. The latter one stands for the damping of the cantilever by the environment. The force gradient approximation, however, fails to account for the nonlinearity of the probe-surface interaction, accordingly, it cannot describe tapping mode operation realistically. A partial solution was presented by Nony *et al.*: assuming a pure sinusoidal motion of the tip, the

time evolution of amplitude and phase signals can be modeled in the form of coupled differential equations.[20,21] This model is applicable to nonlinear interactions, but still excludes dissipative processes like adhesion and viscosity. The literature does not reveal any theoretical works on the analysis of the tapping mode probe bandwidth performed under truly realistic pretenses.

Experimental works on the control of the tapping mode bandwidth were based on Eq. (1). Two main solutions exist: (1) increasing the probe resonance frequency using short cantilevers[22–25] and (2) artificially lowering the effective quality factor of the probe (Q control).[13,26] These solutions, however, introduce additional trade-offs: method (1) requires special optical detection system due to the reduced length of the cantilever[23] thus it cannot be easily adapted to commercial systems, while method (2) is reported to increase the interaction force remarkably.[12,27] None of the two methods provided significantly better imaging results than that can be achieved by expert control of the system parameters,[28] a phenomenon that has not been addressed with scientific scrutiny yet.

The aim of our present work is to perform a comprehensive theoretical and experimental investigation of the dynamical properties of the tapping mode probe. For computer simulation we use a realistic model where we do not apply any restrictions on the tip motion or the tip-sample interaction. Due to the nonlinear nature of the tapping mode probe, a transfer function, commonly used for the characterization of linear systems, cannot be measured, thus we use the describing function method. We show that surface and probe properties can introduce nonlinearities in the amplitude transfer function; that the amplitude of the oscillating probe far from the surface and during operation, and the ratio of the two (setpoint), have a strong influence on the bandwidth, comparable to that of the Q control; and that the theoretical results can be confirmed on a simple commercial AFM system.

II. METHODS

To clarify the terminology that we use in this work, we should distinguish between the stationary (equilibrial) and transient motion of the damped harmonic oscillator, the chosen model of the cantilevered tip system. Previous works frequently discussed "dynamical properties" of the system based on the assumption that it is always in its equilibrial state[2,29,30] having constant amplitude. However, when talking about imaging conditions, this oscillator suffers continuous perturbations from the varying surface topography, a situation which can be described by the nonstationary, i.e., transient solution of the force law. Our work is concerned with the latter situation, accordingly, we use the term "dynamic" to imply to the continuous perturbations by the surface topography, and, intrinsicly, the nonstationary nature of the oscillation.

The describing function (DF) method is commonly used to characterize nonlinear systems.[31] Here, a sinusoidal modulation is applied to the input of the system, and the amplitude and phase transfer corresponding to the applied frequency is determined from the output using Fourier analysis. In case the system is linear, the DF becomes identical to the transfer function. Unlike the transfer function, however, DF may also depend on the modulation amplitude due to the nonlinearity of the system studied. In this work, we both measure and calculate the DF of the AFM probe.

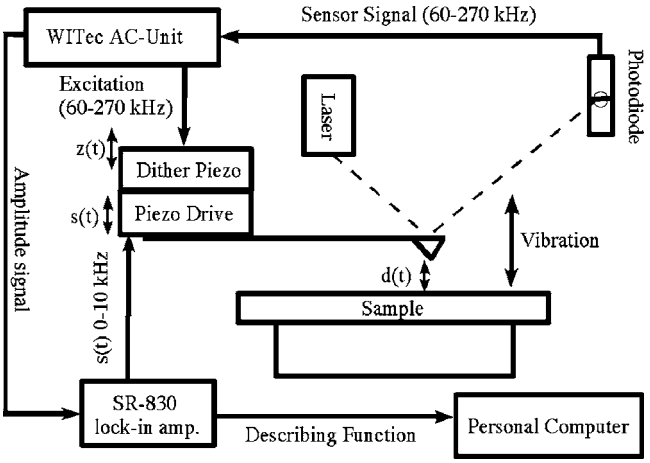

FIG. 1. Block diagram of the experimental arrangement for determining the describing function.

Block diagram of the experimental arrangement used for DF measurements is shown in Fig. 1. Experiments were conducted on a highly oriented pyrolytic graphite sample using Topometrix Explorer and PSIA XE-100 atomic force microscopes. To achieve fast amplitude and phase detection, WITec AC unit, an external high speed digital lock-in amplifier, was used to establish the tapping mode operation instead of the built-in tapping mode controller.[32] The refreshing rate of amplitude and phase measurements was 300 kHz. To measure the DF, the probe-sample distance was modulated by a low frequency sinusoidal signal applied to the vertical (Z) piezo actuator of the AFM scanner, and DF was determined from the amplitude signal output of the WITec AC unit using a separate computer controlled dual phase lock-in amplifier (Stanford Research SR 830). Measurements involved the following steps: (1) the probe was engaged to the surface; (2) the feedback loop gain was minimized to avoid artifacts caused by the AFM controller at measured frequencies; (3) probe-sample distance modulation was introduced and the amplitude response of the AFM was recorded through the lock-in amplifier.

The numerical calculations were based on the point of mass model of the cantilevered tip with a k spring constant.[4] The positions of the tip apex and the piezo drive (the clamped end of the cantilever) are $d(t)$ and $z(t)$, respectively; hence, the deflection of the cantilever is equal to $d(t)-z(t)$. Accordingly, the equation of motion of the tip takes the form

$$\ddot{d}(t) = \omega_0^2[z(t) - d(t)] + \frac{\omega_0}{Q}[\dot{z}(t) - \dot{d}(t)] - \frac{\omega_0^2}{k}F[d(t), \dot{d}(t)], \tag{2}$$

where the $F[d(t), \dot{d}(t)]$ term represents the tip-surface interactions while ω_0 and Q are the same as in Eq. (1). We

chose the Dugdale theory[33] based Maugis continuum mechanics[34,35] $[F_M(d)]$ to describe the contact part of the tip-sample interaction. The benefit of this approach is that it includes not only the nonlinear deformation forces, but also the contact adhesion and adhesion hysteresis. Surface damping $(\beta\dot{d})$ was also included to account for viscoelasticity.[36] In the noncontact region attractive van der Waals forces $[F_{vdW}(d)]$ were assumed,[37] and the matching of the contact and noncontact force curves was established in the same way as in Burnham *et al.*[4] Consistently, the tip-sample interaction force takes the form

$$F(d,\dot{d}) = \begin{cases} F_M(d) + \beta\dot{d}, & \text{contact} \\ F_{vdW}(d), & \text{noncontact.} \end{cases} \quad (3)$$

To simulate the tapping mode, modeling the drive and the amplitude detection process is also required. The first one is implemented through $z(t)$

$$z(t) = Z_0 + s(t) + a_0 \sin(\omega t), \quad (4)$$

where Z_0 represents the time averaged position of the Z piezo drive which was used to establish the desired setpoint amplitude, and Z_0 was constant during the simulation, that is, the surface tracking was disabled. Tapping mode excitation was introduced through a_0 and ω, drive amplitude and angular drive frequency, respectively. The low frequency modulation of the Z piezo drive is modeled by $s(t)$. The probe signal was generated by solving the equation of motion numerically using the fourth order Runge–Kutta method. Evidently, the solution describes only the trajectory traced by the tip; the actual oscillating amplitude of the probe was then determined from the last n periods of the deflection signal using Fourier method, similar to the way the tapping mode controller works.[32] The complex amplitude can be calculated using the formula

$$A(t) = \frac{\omega}{n\pi}\int_0^{2n\pi/\omega} [d(t-\tau) - z(t-\tau)]e^{i\omega(t-\tau)}d\tau. \quad (5)$$

The absolute value and the argument of $A(t)$ yield the amplitude and the phase signals, respectively. To calculate the DF of the system, the probe-sample distance was modulated sinusoidally through $s(t)=S_0 \sin(2\pi ft)$, where f is the modulation frequency of the describing function measurement, and S_0 is the modulation amplitude. Similar to Eq. (5), the describing function $[S(f)]$ was calculated from the amplitude signal $(|A(t)|)$ using

$$S(f) = \frac{2f}{n}\int_0^{n/f} |A(t-\tau)|e^{i2\pi f(t-\tau)}d\tau. \quad (6)$$

III. RESULTS AND DISCUSSION

A. Calculations

DF calculation was performed for ambient tapping mode setup, heretofore referred to as the "basic setup." The following parameters were used: 40 N/m cantilever spring constant, 400 kHz resonance frequency, 10 nm tip radius, 500 as the value of the quality factor, 75 mJ/m^2 adhesion energy, 17 GPa sample Young's modulus and 2×10^{-5} Ns/s surface damping. The cantilever was driven at resonance, and the free and setpoint amplitudes were 50 and 35 nm, respectively. Calculated DF for this setting is shown in Fig. 2. The DF shows a low pass character with nearly constant amplitude transfer at the low frequency region. The associated phase shift increases with the frequency monotonously, however, the slope below the corner frequency is smaller than above it. For accurate, distortion free imaging, the perturbation of the probe should not exceed the corner frequency, 3113 Hz.

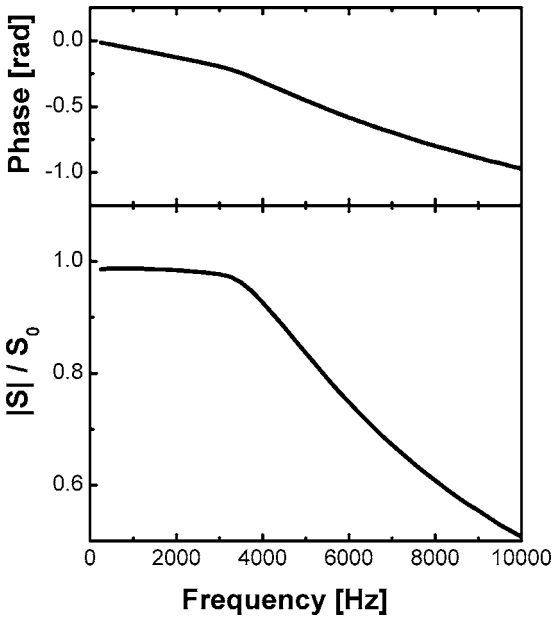

FIG. 2. Calculated describing function of the tapping mode AFM probe in air (basic setup). The following parameters were used: k=40 N/m, $\omega=\omega_0=2\pi\times4\times10^5\frac{1}{s}$, S_0=2 nm, Q=500, 10 nm tip radius, 75 mJ/m^2 adhesion energy, 17 GPa sample Young's modulus and 2×10^{-5} Ns/m surface damping. The free and setpoint amplitudes were 50 and 35 nm, respectively.

For comparison, the −3 dB bandwidth predicted by the force gradient approximation [Eq. (1)] is only 2513 Hz. The calculations also revealed that the corner frequency decreases with increasing modulation amplitude, as expected for a nonlinear system, but the shape of the describing function does not seem to be affected. Consistently, we used 2 nm modulation amplitude (S_0) in the further calculations to maintain comparability.

During the following calculations we investigated the (separate) effects of material and system parameters: the sample adhesion (surface energy), Young's modulus, surface damping and tip radius as well as the quality factor, free and setpoint amplitude of the probe, respectively, on the describing function. Only one parameter was changed in each series of calculations.

The variation of the sample surface energy between 25 and 125 mJ/m^2 caused no significant change but a negligible widening towards higher adhesion in the DF (Fig. 3). This is a somewhat surprising result, knowing that high adhesion is responsible for most height measurement artifacts on the nanometer scale.[8,9]

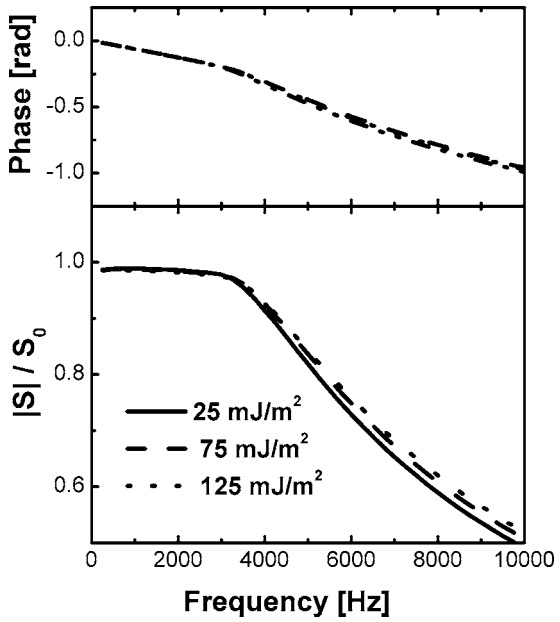

FIG. 3. Effect of adhesion (surface energy of the sample) on the describing function. All other parameters were the same as in the basic setup.

The effect of the Young's modulus of the surface was much more significant: in case of stiff samples (Young's moduli above 100 GPa), not only the bandwidth changes, but also the low frequency amplitude transfer: small peaks indicate the resonant behavior (Fig. 4). The appearance of the peaks is also accompanied by a decrease in the corner frequency.

To include dissipating mechanisms in our study, we investigated the effect of surface damping (Fig. 5). In this case, surface damping gradually decreased from 2×10^{-5} Ns/m to 5×10^{-6} Ns/m. Surprisingly, the conditions favor peaked DFs and lower corner frequency at lower surface damping values (5×10^{-6} Ns/m).

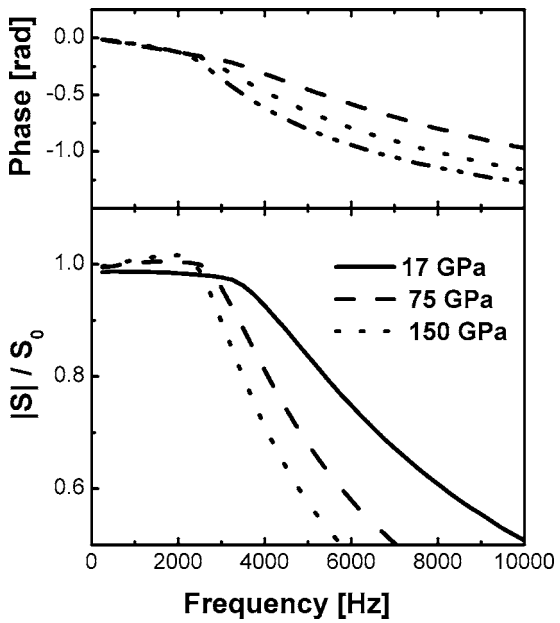

FIG. 4. The effect of the Young's modulus of the surface on the describing function. All other parameters were the same as in the basic setup. Imaging on stiff surfaces reduces the probe bandwidth significantly.

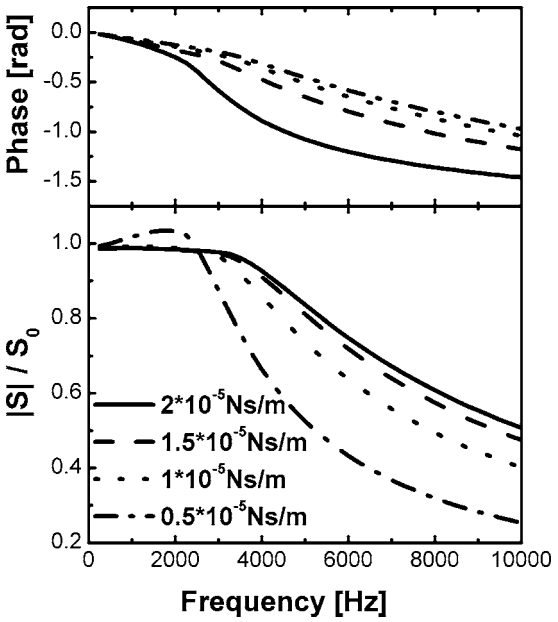

FIG. 5. Effect of surface damping. All other parameters were the same as in the basic setup. At low values (5×10^{-6} Ns/m) a peak can be observed in the amplitude transfer.

Although not explicitly a property of the sample, the tip apex radius strongly influences the force interaction, consistently, we performed calculations in search of a tip effect.

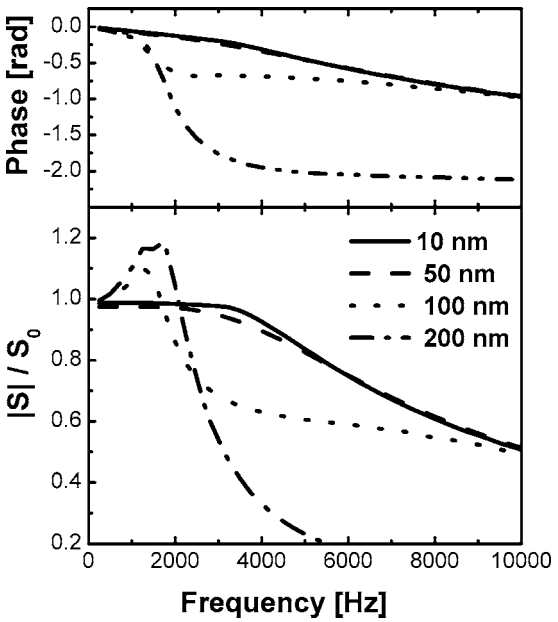

FIG. 6. Effect of tip radius on the describing function. Towards large radii (100–200 nm) a peak develops in the amplitude transfer. This peak is associated with a sudden phase shift. Importantly, both the peak in the amplitude transfer and the phase shift can undermine the stability of the feedback system and could lead to imaging artifacts. All other parameters were the same as in the basic setup.

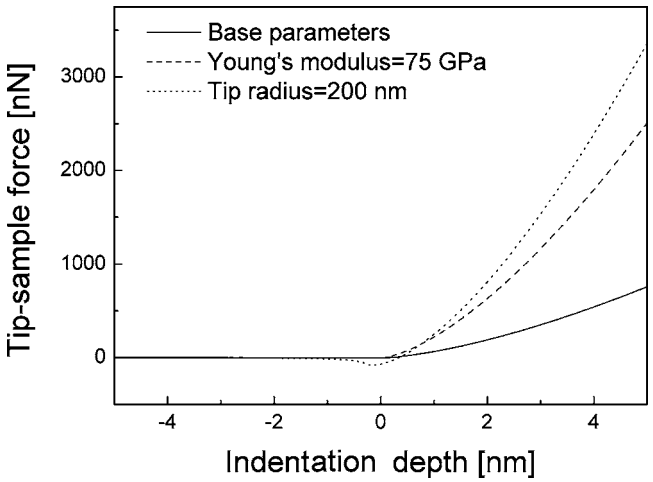

FIG. 7. Tip-sample force as a function of the penetration depth. Calculated for the basic setup (continuous line), for 75 GPa Young's modulus (dashed line), and for 200 nm tip radius (dotted line). The slope of the curve is remarkably higher for high Young's modulus or large tip radius. The increased slope may be responsible for the appearance of peaks in the amplitude transfer function.

Variation of tip radius (Fig. 6) caused remarkable changes in the DF, with large peaks and an abrupt drop in the bandwidth for 100–200 nm (rather blunt) tip apexes. In addition, these changes are accompanied by a sudden phase shift.

We compared the tip-sample interaction force in those cases where peaks appeared to that of the basic setup. It can be seen (Fig. 7) that both large tip radii and high values of Young's moduli result in a steep rise in the maximal exerted force. Hence, indentation depth and tip-sample contact time become significantly shorter, practically, the tip rebound from the surface. This would then lead to "amplification" in the amplitude transfer and, consistently, to the appearance of peaks in the describing function. Naturally, this phenomenon can cause system instabilities. According to the Bode stability criteria of the feedback loop, the phase margin of the system must be positive at the frequency where the open loop gain of the system drops below unity. The enhanced amplitude transfer at the peaks increases the open loop gain while the phase shift decreases the phase margin. Consequently, a blunt tip does not only limit the lateral resolution, but may also be responsible for system instabilities and image distortion.

As we have demonstrated above, dissipating processes, e.g., adhesion and damping, increase the constant amplitude transfer region and consequently the bandwidth of the probe. This result has a special importance for bioimaging where, typically, working in liquid environment provides better quality high resolution images.[38–40] This was implicitly attributed to the better surface tracking due to the reduced quality factor.[23] Our calculations indicate that besides the reduced quality factor, increased attractive forces (e.g., hidrophobicity) and surface damping may also lead to higher stability due to the wider linear amplitude transfer in the damping medium.

Turning our attention to the probe properties, first we investigated the effect of the quality factor. Lowering Q from

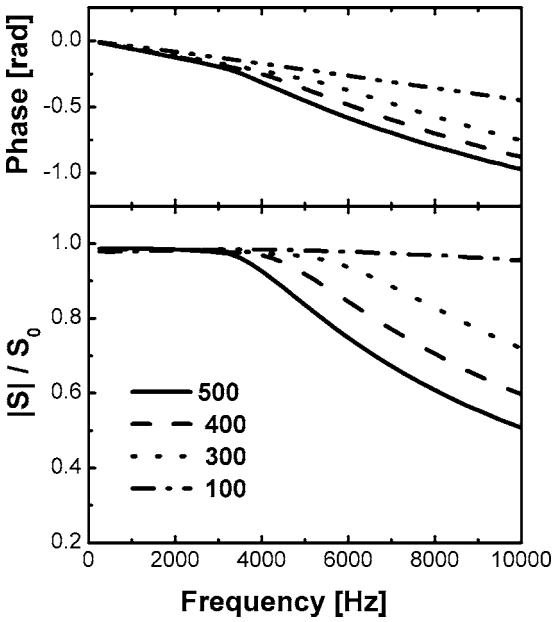

FIG. 8. Effect of the quality factor (Q) on the DF. In accordance with the classical theory, lowering the quality factor increases the corner frequency and thus the probe bandwidth.

500 to 400, 300 and finally 100 (Fig. 8) resulted in a gradually increasing bandwidth, in accordance with the predictions of the force gradient approximation [Eq. (1)].

Influence of the free amplitude has been investigated while the setpoint is set to 70% of the actual free amplitude (Fig. 9) and also when the setpoint amplitude was fixed to 35 nm (Fig. 10). Surprisingly, we found that the DF is very

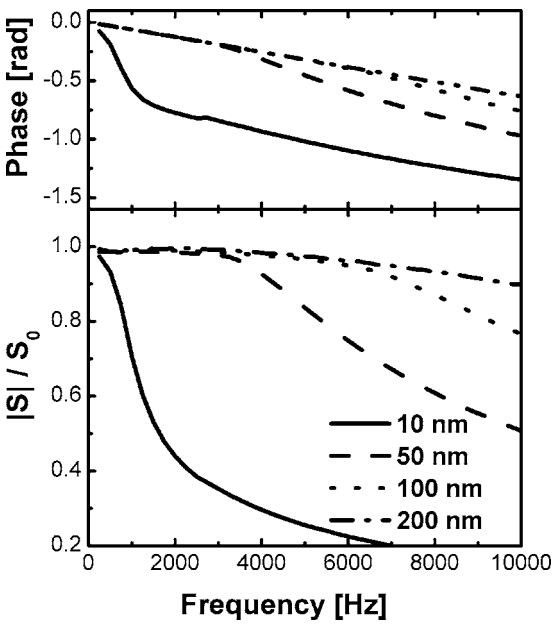

FIG. 9. Effect of the free oscillating amplitude of the probe on the describing function at constant setpoint free amplitude ratio. The setpoint amplitude was 70% of the actual free amplitude. All the other parameters were set to basic setup values. These graphs show that a slight increase of the free amplitude widens the probe bandwidth remarkably.

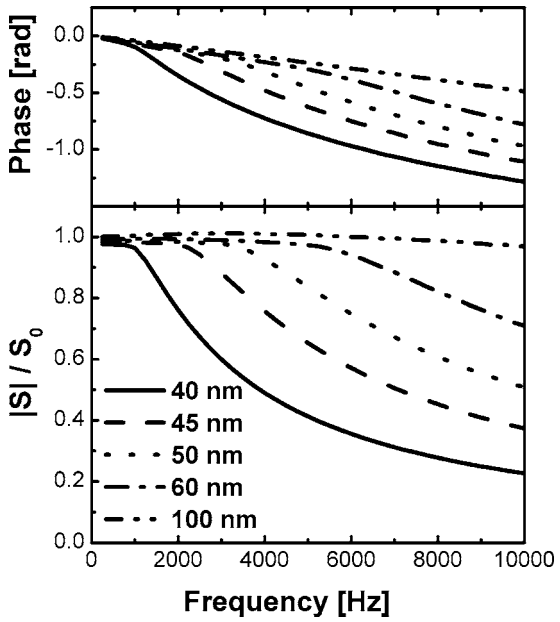

FIG. 10. Effect of the free oscillating amplitude of the probe on the describing function at constant setpoint amplitude. The setpoint amplitude was constant (35 nm) and the free amplitude was varied between 40 and 100 nm. All the other parameters were set to basic setup values.

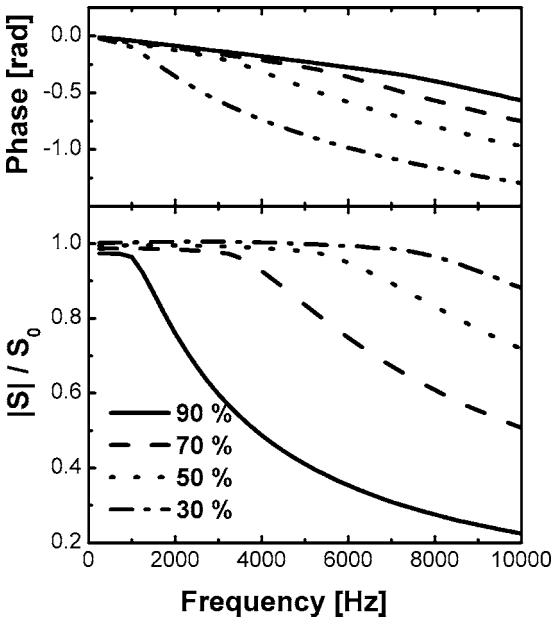

FIG. 11. Effect of the setpoint amplitude on the describing function. During these calculations the free amplitude was 50 nm and all other parameters corresponded to basic setup values. It can be seen that lower setpoint values can increase the bandwidth of the probe.

sensitive even to slight changes of the free amplitude. For comparison, the force gradient approximation would not predict any such sensitivity.[13] Comparing Figs. 9 and 10 with Fig. 8, it is apparent that increasing the free amplitude widens the probe bandwidth comparably to lowering Q from 500 to 100. Consistently, the free amplitude appears to be just as an effective tuning parameter of the tapping mode probe bandwidth as the quality factor.

Based on above results it is a straightforward assumption that the setpoint amplitude may also have an influence on the DF. Indeed, lowering the setpoint amplitude from 45 to 15 nm (at 50 nm free amplitude) resulted in a five times higher corner frequency (Fig. 11). Hence, in addition to the quality factor and the free amplitude, the setpoint amplitude can also be used for tuning the imaging bandwidth.

B. Experiments

To test the predictions of the numerical results, we performed experiments with two AFM systems using the setup shown on Fig. 1. In a commercial AFM, recording the DF at high frequencies is problematic due to built-in low pass filters and hardware bandwidth limits. One way to overcome this limitation is using low resonance "soft tapping" probes. Describing functions were recorded with a Topometrix Explorer AFM operating on graphite surface at 25, 50 and 67 nm free amplitudes (Fig. 12). The setpoint amplitude was 20 nm for all cases. It can be seen that, in a good agreement with the calculations (Fig. 10), increasing the free amplitude leads to wider probe bandwidth.

An alternative way to demonstrate the dynamic effects is the application of high modulation amplitudes, a situation when the corner frequency is conveniently lower. We used PSIA XE-100 atomic force microscope with standard tapping cantilever. The probe-surface modulation was 18.3 nm. These conditions are as close as we could get to the parameters of the calculations on a commercial AFM system. Re-

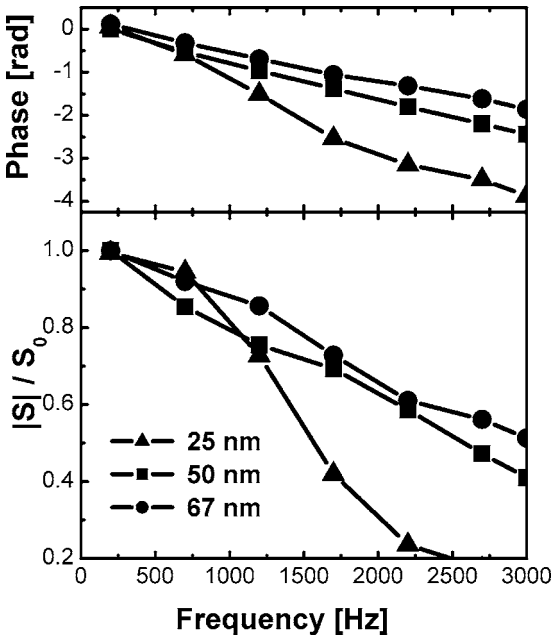

FIG. 12. Experimental DF curves taken on graphite surface with varied free amplitudes: 25 nm (▲), 50 nm (■), 67 nm (●). All other parameters were maintained constant. Cantilever resonance frequency, quality factor and nominal spring constant were 60 172 Hz, 120 and 1.0 N/m, respectively. The setpoint amplitude was 20 nm. The solid lines are guides for eyes.

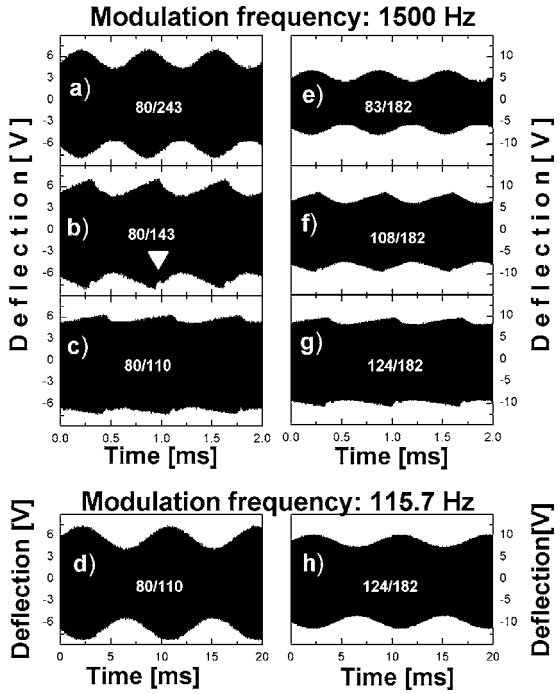

FIG. 13. Effect of the free amplitude and setpoint on the amplitude transfer of a tapping mode AFM probe (40 N/m nominal spring constant, 316.85 kHz resonance frequency) when exposed to periodic topography perturbations. The probe-surface distance was modulated by a 18.3 nm 1500 Hz [panels (a)–(c), and (e)–(g)] and 115.7 Hz [panels (d), (h)] sinusoidal signal. Feedback was inactive. Left Panels: free amplitudes were 243 nm (a), 143 nm (b), 110 nm (c), and 110 nm (d). The setpoint was 80 nm. Right panels: setpoint amplitudes were 83 nm (e), 108 nm (f), 124 nm (g), and 124 nm (h) with a constant 182 nm free amplitude. Note the distortion of the signal at low free amplitues and high setpoints.

sults are depicted in Fig. 13. During these experiments only the setpoint and free amplitudes were changed, any other parameters were constant and the topography feedback loop was inactive. Setpoint amplitude was monotonously increased in Figs. 13(e)–13(g) while the free amplitude was decreased in Figs. 13(a)–13(c). Alteration of both parameters leads to remarkably smaller observable modulation depth in the cantilever deflection signal which is in accordance with the calculations (Figs. 10 and 11). Small glitches can be seen at negative deflection values (Fig. 13, $\bigtriangledown$) which can be explained as follows. At high frequency, the probe amplitude cannot increase at the rate of the probe surface separation, thus the probe loses contact with the surface. A half period later, the probe approaches the surface and the intermittent contact reinstated. The glitches observable in the figure show the points of these transitions. Control experiments [Figs. 13(d)–13(h)] performed at one order of magnitude lower modulation frequency do not show any glitches or reduced transference, clearly indicating that the observed phenomena originate from a dynamic effect. Note, in the experiments the quality factor and drive frequency were constant and under these conditions the force gradient approximation does not predict any change in the probe bandwidth, that is, based on previously published theories no change of the transference is predicted.

IV. CONCLUSION

We performed a comprehensive experimental and computational study of the imaging bandwidth of the tapping mode AFM using describing function method. We have shown that, for a wide range of parameters, the low frequency amplitude transfer is linear and the corner frequency is higher than predicted by linear models. Consistently, the dynamical range of distortion-free imaging is larger than expected. We established that dissipating processes like adhesion, surface and environmental damping increase the probe bandwidth. We also found that steep gradients of the interaction force, as in the case of using blunt tips or imaging stiff surfaces, cause peaking in the describing function and decrease the bandwidth. Consistently, experimentally observed system instabilities and image distortion during high resolution imaging with tips of large radii, usually attributed to tip convolution, can be also caused by nonlinear probe behavior. We demonstrated that the free and setpoint amplitudes of the probe during tapping operation are sensitive controls of probe bandwidth; thus, careful selection of the working parameters can be as effective as active probe quality control ("Q control") in improving image quality. These results provide a theoretical background for the empirical observations of a generation of AFM operators.

ACKNOWLEDGMENTS

Financial support from the TS049872 and TO46394 Grants of the Hungarian Scientific Research Found (OTKA), Grant No. of NKFP 3AP/071/2004 from the Hungarian Ministry of Culture and Education, and Australian Research Council Discovery Grants No. DP0662816 and No. DP0663290 are kindly acknowledged. J.K. expresses his sincere gratitude to the German Academic Exchange Service (DAAD) for his scholarship. A.M. gratefully acknowledges his support from the Swedish Foundation for International Cooperation in Research and Higher Education (STINT), and Monash University. The authors would like to thank Z. L. Horváth for his contribution to this work and WITec GmbH for their technical assistance.

*Permanent address: Institute for Engineering and Materials Science, University of Szeged, P.O. Box: 406, H-6701 Szeged, Hungary.

†Permanent address: Research Group on Laser Physics of the Hungarian Academy of Sciences, P.O. Box: 406, H-6701 Szeged, Hungary.

[1] G. Binnig, C. F. Quate, and C. Gerber, Phys. Rev. Lett. **56**, 930 (1986).

[2] B. Anczykowski, D. Krüger, and H. Fuchs, Phys. Rev. B **53**, 15485 (1996).

[3] J. Berg and G. A. D. Briggs, Phys. Rev. B **55**, 14899 (1997).

[4] N. A. Burnham, O. P. Behrend, F. Oulevey, G. Gremaud, P.-J.

Gallo, D. Gourdon, E. Dupas, A. J. Kulik, H. M. Pollock, and G. A. D. Briggs, Nanotechnology **8**, 67 (1997).
[5] A. Kühle, A. H. Sorensen, J. B. Zandbergen, and J. Bohr, Appl. Phys. A **66**, S329 (1998).
[6] O. P. Behrend, F. Oulevey, D. Gourdon, E. Dupas, A. J. Kulik, G. Gremaud, and N. A. Burnham, Appl. Phys. A **66**, S219 (1998).
[7] R. Garcia and A. San Paulo, Ultramicroscopy **82**, 79 (2000).
[8] A. Mechler, J. Kokavecz, P. Heszler, and R. Lal, Appl. Phys. Lett. **82**, 3740 (2003).
[9] A. Mechler, J. Kopniczky, J. Kokavecz, A. Hoel, C. G. Granqvist, and P. Heszler, Phys. Rev. B **72**, 125407 (2005).
[10] G. Schitter, P. Menold, H. F. Knapp, F. Allgöver, and A. Stemmer, Rev. Sci. Instrum. **72**, 3320 (2001).
[11] T. Sulchek, G. G. Yaralioglu, C. F. Quate, and S. C. Minne, Rev. Sci. Instrum. **73**, 2928 (2002).
[12] J. Kokavecz, P. Heszler, Z. Tóth, and A. Mechler, Appl. Surf. Sci. **210**, 123 (2003).
[13] J. Mertz, O. Marti, and J. Mlynek, Appl. Phys. Lett. **62**, 2344 (1993).
[14] H.-J. Nam, Y.-S. Kim, S.-M. Cho, C. S. Lee, J.-U. Bu, J.-W. Hong, and Z.-G. Khim, J. Appl. Phys. **41**, 7153 (2002).
[15] S. R. Manalis, S. C. Minne, A. Atalar, and C. F. Quate, Rev. Sci. Instrum. **67**, 3294 (1996).
[16] S. R. Manalis, S. C. Minne, and C. F. Quate, Appl. Phys. Lett. **68**, 871 (1996).
[17] S. R. Manalis, S. C. Minne, A. Atalar, and C. F. Quate, Appl. Phys. Lett. **69**, 3944 (1996).
[18] G. Schitter, F. Allgöver, and A. Stemmer, Nanotechnology **15**, 108 (2004).
[19] G. E. Fantner, P. Hegarty, J. H. Kindt, G. Schitter, G. A. G. Cidade, and P. K. Hansma, Rev. Sci. Instrum. **72**, 026118 (2005).
[20] L. Nony, R. Boisgard, and J.-P. Aimé, J. Chem. Phys. **111**, 1615 (1999).
[21] L. Nony, R. Boisgard, and J.-P. Aimé, Eur. Phys. J. B **24**, 221 (2001).
[22] A. R. Hodges, K. M. Bussmann, and J. H. Hoh, Rev. Sci. Instrum. **72**, 3880 (2001).
[23] M. B. Viani, T. E. Schäffer, G. T. Paloczi, L. I. Pietrasanta, B. L. Smith, J. B. Thompson, M. Richter, M. Rief, H. E. Gaub, K. W. Plaxco, A. N. Cleland, H. G. Hansma, and P. K. Hansma, Rev. Sci. Instrum. **70**, 4300 (1999).
[24] D. A. Walters, J. P. Cleveland, N. H. Thomson, P. K. Hansma, M. A. Wendman, G. Gurley, and V. Elings, Rev. Sci. Instrum. **67**, 3583 (1996).
[25] T. Ando, N. Kodera, E. Takai, D. Maruyama, K. Saito, and A. Toda, Proc. Natl. Acad. Sci. U.S.A. **98**, 12468 (2001).
[26] T. Sulchek, R. Hsieh, J. D. Adams, G. G. Yaralioglu, S. C. Minne, C. F. Quate, J. P. Cleveland, A. Atalar, and D. M. Adderton, Appl. Phys. Lett. **76**, 1473 (2000).
[27] B. Anczykowski, J. P. Cleveland, D. Krüger, V. Elings, and H. Fuchs, Appl. Phys. A: Mater. Sci. Process. **66**, S885 (1998).
[28] R. D. Jäggi, A. Franco-Obrégon, P. Studerus, and K. Ensslin, Appl. Phys. Lett. **79**, 135 (2001).
[29] A. S. San Paulo and R. Garcia, Phys. Rev. B **66**, 041406 (2002).
[30] P. J. dePablo, J. Colchero, M. Luna, J. Gómez-Herrero, and A. M. Baró, Phys. Rev. B **61**, 14179 (2000).
[31] M. Gopal, *Modern Control System Theory* (Wiley, New York, 1993).
[32] P. Spizig (private communication).
[33] D. S. Dugdale, J. Mech. Phys. Solids **8**, 100 (1960).
[34] D. Maugis, J. Colloid Interface Sci. **150**, 243 (1992).
[35] D. Maugis and B. Gauthier-Manuel, J. Adhes. Sci. Technol. **8**, 1311 (1994).
[36] R. G. Winkler, J. P. Spatz, S. Sheiko, M. Möller, P. Reineker, and O. Marti, Phys. Rev. B **54**, 8908 (1996).
[37] J. N. Israelechvili, *Intermolecular and Surface Forces* (Academic, London, 1991).
[38] R. Lal, S. A. John, D. W. Raird, and M. F. Arnsdorf, Am. J. Physiol.: Cell Physiol. **268**, 968 (1995).
[39] L. I. Pietrasanta, D. Thrower, W. Hsieh, S. Rao, O. Stemmann, J. Lechner, J. Carbon, and H. Hansma, Proc. Natl. Acad. Sci. U.S.A. **96**, 3757 (1999).
[40] F. Oesterhelt, D. Oesterhelt, M. Pfeiffer, A. Engel, H. E. Gaub, and D. J. Muller, Science **288**, 143 (2000).